

In-depth studies of the NGC 253 ULXs with XMM-Newton: remarkable variability in ULX1, and evidence for extended coronae

R. Barnard¹

¹*Department of Physics and Astronomy, The Open University, Walton Hall, Milton Keynes, MK7 6AA, UK*

ABSTRACT

We examined the variability of three ultra-luminous X-ray sources (ULXs) in the 2003, 110 ks XMM-Newton observation of NGC 253. Remarkably, we discovered ULX1 to be three times more variable than ULX2 in the 0.3–10 keV band, even though ULX2 is brighter. Indeed, ULX1 exhibits a power density spectrum that is consistent with the canonical high state or very high/steep power law states, but not the canonical low state. The 0.3–10 keV emission of ULX1 is predominantly non-thermal, and may be related to the very high state. We also fitted the ULX spectra with disc blackbody, slim disc and convolution Comptonization (SIMPL \otimes DISKBB) models. The brightest ULX spectra are usually described by a two emission components (disc blackbody + Comptonized component); however, the SIMPL model results in a single emission component, and may help determine whether the well known soft excess is a feature of ULX spectra or an artifact of the two-component model. The SIMPL models were rejected for ULX3 (and also for the black hole + Wolf-Rayet binary IC10 X-1); hence, we infer that the observed soft-excesses are genuine features of ULX emission spectra. We use an extended corona scenario to explain the soft excess seen in all the highest quality ULX spectra, and provide a mechanism for stellar mass black holes to exhibit super-Eddington luminosities while remaining locally sub-Eddington.

Key words: X-rays: general – X-rays: binaries – Galaxies: individual: NGC 253 – black hole physics

1 INTRODUCTION

In Barnard et al. (2008a) we identified a new spectral state in the confirmed black hole + Wolf-Rayet binary IC10 X-1, as well as the BH+WR candidate NGC 300 X-1 and the well known black hole binary LMC X-1. Both IC10 X-1 and NGC 300 X-1 exhibited ~ 0.0001 – 0.1 Hz power density spectrum (PDS) where the power is inversely proportional to the frequency, like the canonical high state. However, the 0.3–10 keV for these sources emission is predominantly non-thermal, while the canonical emission spectrum for high state black hole X-ray binaries is dominated by a multi-temperature disk blackbody that contributes $\sim 90\%$ of the 1–10 keV flux (McClintock & Remillard 2006).

In Barnard et al. (2008a) we proposed that the non-thermal high state was due to a persistently high accretion rate maintaining a stable corona; most black hole X-ray binaries are transient, and we suggested that the canonical soft high state was caused by the ejection of the corona during outburst. After finding out from Soria & Kuncic (2008) that $\sim 90\%$ of X-ray sources with luminosities $>10^{39}$ erg s^{−1} have non-thermal spectra, we suggested that the same phys-

ical processes may apply in these sources as in IC10 X-1 and NGC 300 X-1. The ultra-luminous X-ray sources (ULXs) are an intriguing class of extragalactic X-ray sources that are not associated with the galaxy nucleus, yet exhibit X-ray luminosities $>2\times 10^{39}$ erg s^{−1}, the Eddington limit for a $\sim 15 M_{\odot}$ black hole (see e.g. Roberts 2007, for a review).

Our survey of X-ray sources in the 2003 XMM-Newton observation of the nearby spiral galaxy NGC 253 (Barnard et al. 2008b) yielded three X-ray sources with 0.3–10 keV luminosities $>2\times 10^{39}$ erg s^{−1}. We shall call these ULX1–ULX3, and their known properties are presented in Table 1; these properties are taken from our survey (Barnard et al. 2008b). In this paper, we examine the variability of these sources. We also perform additional spectral fitting; we model their spectra with slim disc models, and “physical” Comptonization models where the inner disc provides the seed photons. In Section 2 we discuss the observation and data analysis, followed by the results in Section 3. Our discussion and conclusion is presented in Section 4.

1.1 ULX variability

Few ultra-luminous X-ray sources (ULXs) have sufficiently high quality data for timing analysis. The PDS of M82 X-1 has been characterised by a quasi-periodic oscillations (QPOs) at 54 mHz (Strohmayer & Mushotzky 2003) and 114 Hz (Dewangan et al. 2006b), on top of a broken power law continuum (Dewangan et al. 2006b). QPOs have also been found in Holmberg IX X-1 (along with a power law continuum Dewangan et al. 2006a) and NGC 5408 X-1 (with a broken power law continuum Strohmayer et al. 2007).

Heil et al. (2009) conducted a timing study of ULXs observed with XMM-Newton. They analysed 19 observations of 16 ULXs and found 6 ULXs with PDS best described by power laws or broken power laws: M82 X-1, NGC 1313X-1, NGC 1313 X-2, NGC 55 ULX, Ho IX X-1 and NGC 5408 X-1; the others showed no significant variability. Heil et al. (2009) obtained upper limits to the variability of these ULXs, and concluded that the intrinsic variability was lower.

1.2 ULX emission spectra

Two emission components are often used to describe the X-ray spectra of ULXs: a thermal component, and a component, e.g. power law, to represent inverse Compton scattering of cool photons on hot electrons. (see e.g. Stobbart et al. 2006; Gladstone et al. 2009). These fits often result in a “soft excess”, where the power law component diverges from the thermal component. Such spectra have been deemed by some as non-standard and unphysical, assuming that the seed photons are provided by the inner disc (see e.g. Roberts et al. 2005; Gonçalves & Soria 2006).

Gladstone et al. (2009) conducted a survey of XMM-Newton observations of ULXs with >10000 source counts in their EPIC spectra; their preferred model consists of a disc blackbody and a Comptonized component with the seed photons tied to the inner disc temperature. They found two universal features: a soft excess and roll-over in the spectrum above ~ 3 keV. They found that disc + Comptonized corona emission models fitted the data well; however, the resulting coronae were cool ($kT \simeq 1\text{--}3$ keV) and optically thick ($\tau \sim 5\text{--}30$). The combination of a cool disc and broken hard component led Gladstone et al. (2009) to define a new, ultraluminous spectral state. Such coronae are distinct from coronae of Galactic binaries ($\tau \sim 1$), and Gladstone et al. (2009) use this difference to reject the scenario of sub-Eddington accretion onto intermediate mass black holes.

2 OBSERVATION AND ANALYSIS

In Barnard et al. (2008b) we conducted a spectral survey of X-ray sources in the 2003 XMM-Newton observation of NGC 253; full details of our data reduction are given in that paper. The present work concerns new variability studies of three ULXs. In Barnard et al. (2007) we showed that the combination of lightcurves from the different cameras on-board XMM-Newton can lead to artefacts in the PDS. To ensure fidelity of the PDS, we performed our variability analysis on the unbinned pn events files for each source. The total exposure time was ~ 110 ks; however, several background

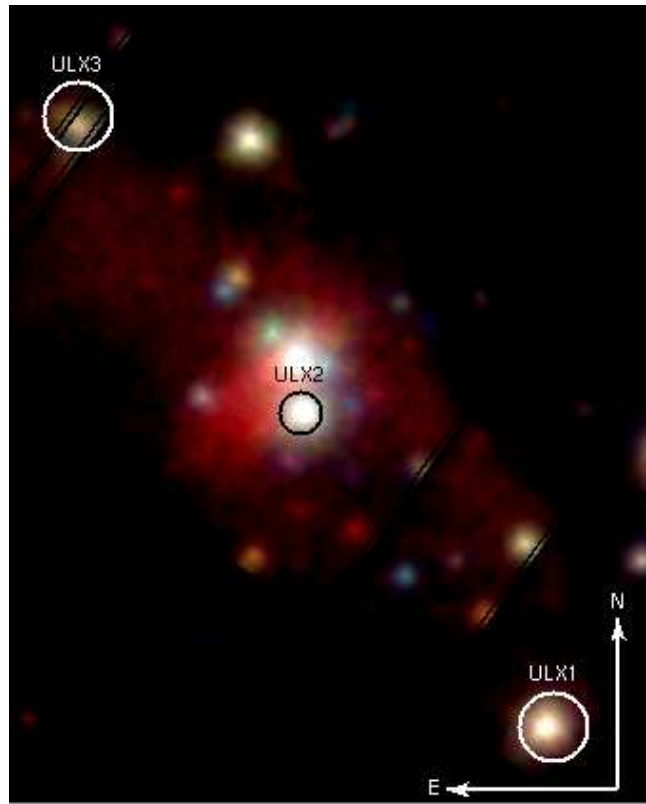


Figure 1. Detail of a three colour pn + MOS image of NGC 253 showing ULX1, ULX2 and ULX3. Red represents 0.3–2.0 keV, green represents 2.0–3.0 keV, and blue represents 4.0–10 keV. The image is log-scaled, and the source extraction regions for the ULXs are labeled.

flares occurred during the observation; the flares were removed (see Barnard et al. 2008b, for details), leaving ~ 50 ks of good data.

3 RESULTS

Figure 1 shows a three colour detail of the combined EPIC (pn + MOS1 + MOS2) image of NGC 253, overlaid with the source extraction regions; the image is log-scaled, north is up and east is left.

3.1 Variability

We present the 0.3–10 keV pn lightcurves of ULX1, ULX2 and ULX3 in Figure 2, binned to 100 s from the unbinned events. Intervals with strong background flares have been filtered out. The background contribution is negligible in each case. The x- and y-axes are plotted on the same scale for each source. For each lightcurve we provide the fractional r.m.s. variability calculated by the program LCURVE from the FTOOLS analysis suite¹. We note that ULX3 is rather fainter than ULX1 and ULX2 and there are two reasons for this. Firstly, ULX3 is located at the corner of a chip in the pn image, and the collecting area is reduced when the

¹ http://heasarc.nasa.gov/lheasoft/ftools/ftools_menu.html

Table 1. Known properties of the three ULXs, taken from our survey of X-ray sources in NGC 253 (Barnard et al. 2008b). For each source we give the source coordinates as returned by the source detection routine; these have uncertainties of $\sim 2''$. We then give the number of net source counts in pn and MOS detectors. Next we give the details of the best fit spectral model: absorption (N_H), blackbody temperature (kT) and photon index (Γ), along with the corresponding χ^2/dof and 0.3–10 keV luminosity / 10^{39} erg s $^{-1}$. Numbers in parentheses indicate 90% confidence limits on the final digit.

Source	Position	pn	MOS	$N_H/10^{21}$ atom cm $^{-2}$	kT/keV	Γ	χ^2/dof	$L/10^{39}$
ULX1	00 47 22.56 –25 20 51	10537	10390	2.00(2)	0.73(5)	2.14(4)	347/323	2.90(12)
ULX2	00 47 32.98 –25 17 50	11614	12014	2.9(2)	0.98(6)	1.94(5)	374/374	4.10(19)
ULX3	00 47 42.41 –25 14 59	773	4156	6.0(11)	0.94(8)	3.4(5)	84/76	2.4(4)

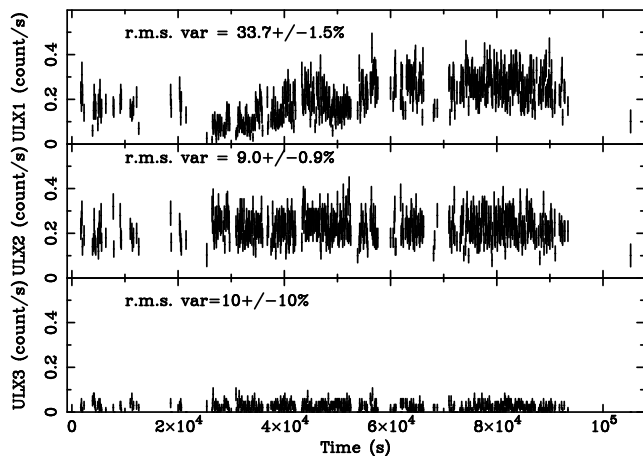


Figure 2. Lightcurves of the three ULXs, binned to 100 s from the unbinned 0.3–10 keV pn events. X- and y- axes are set to the same scales. We give the fractional r.m.s. variability of each lightcurve.

(FLAG==0) filter is applied; lastly, ULX3 is more heavily absorbed than the other two. ULX1 is particularly variable, ranging in intensity over ~ 0.0 – 0.4 count s $^{-1}$; analysis of the ULX1 lightcurves in the 0.3–2.5 keV and 2.5–10 keV bands showed no evidence for energy dependence in this variability.

For each source, we constructed 0.3–10 keV PDS that were averaged over several intervals consisting of 64 bins with a resolution of 100 s; intervals of background flaring were excluded. Figure 3 shows the resulting PDS for ULX1 (black) and ULX2 (grey), which have comparable intensities. The PDS are normalized to give the $(\text{r.m.s.}/\text{mean})^2$ power and the expected noise is subtracted; the PDS are binned by to give 56 frequencies per bin. The PDS of ULX1 (black) is well described by a power law; if the power at frequency ν is $P(\nu)$, then $P(\nu) \propto \nu^{-\gamma}$. We show the best fit power law to the ULX1 PDS in Fig. 3; $\gamma = 1.0 \pm 0.5$, with $\chi^2/\text{dof} = 3$ for 6 degrees of freedom (dof). Fitting the ULX1 PDS with zero power yields $\chi^2/\text{dof} = 26/8$, an unacceptable fit; hence the observed power in ULX1 is significant. The PDS for ULX2 shows no strong evidence for variability, even though ULX2 is slightly brighter than ULX1; fitting zero power to the ULX2 PDS yields $\chi^2/\text{dof} = 5/6$. Hence the observed power from ULX1 is intrinsic, rather than an artefact of the observation. Indeed, the PDS of the combined pn+MOS1+MOS2 lightcurves of ULX2 and ULX3 were also featureless. These results show that 10,000 source counts are

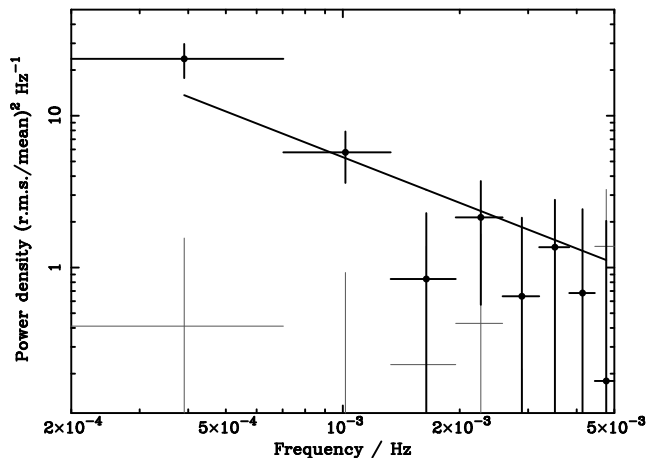


Figure 3. Power density spectra constructed from 0.3–10 keV pn events for ULX1 (black) and ULX2 (grey); the expected noise is subtracted. The PDS of ULX1 features strong variability at low frequencies; we provide the best fit power law model with $\gamma = 1.0 \pm 0.5$ ($\chi^2/\text{dof} = 3/6$).

sufficient for detecting $\gamma \sim 1$ PDS in sources where the r.m.s. variability is $\sim 30\%$, but not for sources with 10% variability.

The frequency range of our PDS is $\sim 2 \times 10^{-4}$ – 5×10^{-3} Hz. Churazov et al. (2001) showed that Cygnus X-1 exhibits similar power law noise with $\gamma \sim 1$ in this frequency range during its low state and high state; however, the r.m.s.² power of Cygnus X-1 at $\sim 10^{-4}$ Hz is ~ 20 times higher in the high state than in the low state. This is unsurprising, because the high state PDS is characterised by a $\gamma \sim 1$ power law over the 0.0001–10 Hz range, while its low state is similar, except for the interval $\sim 2 \times 10^{-3}$ – 2×10^{-1} Hz where $\gamma \sim 0$. The variability of ULX1 is consistent with that of Cygnus X-1 in the high state, but not its low state.

We compared the 10^{-2} –10 Hz PDS of Cygnus X-1 in the high and low states (Churazov et al. 2001), with the 10^{-2} –10 Hz PDS of other black hole X-ray binaries in the high, low and steep power law states (McClintock & Remillard 2006). The high state PDS of Cygnus X-1 has rather more power at 10^{-2} Hz than the high states of other black hole binaries; this may be a consequence of its high mass donor. The low state PDS of Cygnus X-1 shows variability at 10^{-2} Hz that is as high as, or higher than the PDS of other black holes in the low state. It is difficult to distinguish between the high and very high states variability alone; we therefore infer that ULX1 is in a high accretion rate state that may be related to the high or very high/ state.

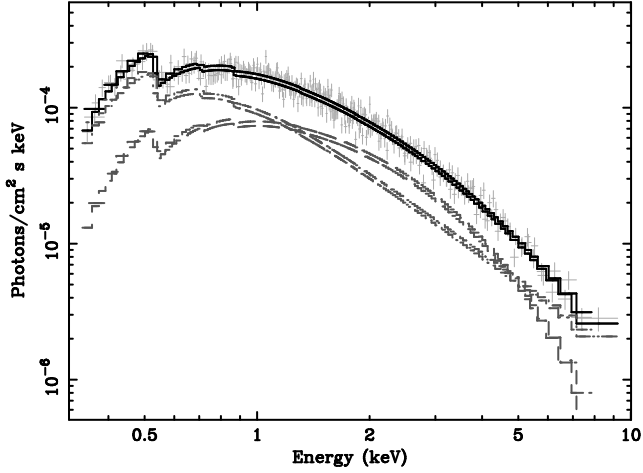


Figure 4. Unfolded 0.3–10 keV pn and combined MOS spectra of ULX1, modelled with disc blackbody and power law emission components, and suffering photo-electric absorption by material in the line of sight. A constant of normalization accounts for the differences in pn and MOS responses.

3.2 Spectral analysis

The emission spectra of the brightest ULXs are generally well described by disc emission plus a Comptonization component (see e.g. Stobbart et al. 2006). Figure 4 shows the unfolded 0.3–10 keV pn and spectrum of ULX1, simultaneously modeled with a disc blackbody and a power law component to represent Comptonization; line-of-sight absorption is included, and a constant of normalization accounts for differences in the pn and MOS responses. The Comptonized component contributes most of the 0.3–10 keV emission; however, the thermal emission dominates the ~ 1 –5 keV range. The power law component dominates the spectrum below ~ 1 keV; this “soft excess” is sometimes deemed unphysical, as the seed photons for the Comptonization are assumed to come from the inner disc (see e.g. Roberts et al. 2005; Gonçalves & Soria 2006). In this section, we model the spectra of ULX1–ULX3 with several alternative models.

3.2.1 Disc blackbody models

The emission spectra of distant ULXs are often successfully described by disc blackbody models (see e.g. Isobe et al. 2009). However, for these models to be meaningful, they must have inner disc temperatures and luminosities that are consistent with the black hole mass, M_{BH} ; the temperature is governed by $M_{\text{BH}}^{-1/4}$, while the luminosity should not exceed $\sim 0.5 L_{\text{Edd}}$ (Mitsuda et al. 1984).

Successful fits to the NGC253 ULX spectra with meaningful disc blackbody models would indicate that these systems were in the canonical high state; disc temperatures range over ~ 0.7 – 1.5 keV for most known black hole binaries in the high state (McClintock & Remillard 2006). Therefore we simultaneously fitted absorbed disc blackbody models to the pn and combined MOS spectra for each ULX; a constant of normalisation is included to account for differences in the pn and MOS responses. We reject the absorbed disc blackbody model for ULX1 and ULX3. The disc blackbody fit for ULX2 is acceptable: $N_{\text{H}} = 1.56 \pm 0.08 \times 10^{21}$ atom cm^{-2} , kT_{in}

$= 1.68 \pm 0.04$ keV, and $\chi^2/\text{dof} = 397/376$ (good fit probability, g.f.p. = 0.22). However, the temperature for ULX2 is rather higher than known black hole binaries, and is inconsistent with the modelled 0.3–10 keV luminosity of 3×10^{39} erg s^{-1} . F-testing shows the blackbody + power law model to be a better fit; the probability that this improvement is due to chance is 1.4×10^{-5} .

3.2.2 Slim disc models

Slim disc models have also been applied to some ULXs (see e.g. Okajima et al. 2006). Kawaguchi (2003) provides a suite of tabular models for XSPEC¹, including a standard disc, thermal and Comptonized slim discs, with and without relativistic effects. Each model is described by four parameters; the mass of the accretor, M , is given in solar masses; the accretion rate, \dot{M} , is normalised to L_{Edd}/c^2 , so that Eddington accretion corresponds to $\dot{M} \simeq 10$ (Kawaguchi 2003); the viscosity parameter, α , is limited to the range 0.01–1; the normalisation is defined as $(10 \text{ kpc}/d)^2$, where d is the distance. The distance was fixed to 4 Mpc, following Grimm et al. (2003).

We applied these slim disc models to our ULX targets. For ULX1, no thermal model resulted in good fits, meaning that Comptonization was required. The best results were gleaned from the Comptonized slim disc model with relativistic correction: $N_{\text{H}} = 1.53 \pm 0.06 \times 10^{21}$ atom cm^{-2} , $M = 17.5 \pm 1.5 M_{\odot}$, $\dot{M} = 12.8 \pm 0.8 L_{\text{Edd}}/c^2$, $\alpha = 0.11 \pm 0.03$, and $\chi^2/\text{dof} = 351/324$ (g.f.p. = 0.14). For ULX2, all slim disc models failed, with g.f.p. $< 2 \times 10^{-6}$. ULX3 was best described by a modified blackbody with relativistic correction: $N_{\text{H}} = 3.7 \pm 0.2 \times 10^{21}$ atom cm^{-2} , $M = 8 \pm 7 M_{\odot}$, $\dot{M} = 10.7 \pm 0.7 L_{\text{Edd}}/c^2$, $\alpha = 0.36 \pm 0.10$, $\chi^2/\text{dof} = 94/77$ (g.f.p. = 0.09). F-testing showed that our two-component model has a 99.6% probability of providing a significant improvement.

3.2.3 Self-consistent Comptonization of a disc blackbody

Steiner et al. (2008) have produced a convolution model for XSPEC v12, SIMPL, which describes the Comptonization of any input spectrum; the modeling can include up-scattering and down-scattering, or upscattering only. It uses only two free parameters: the photon index of the resulting power law, and the fraction of scattered photons. Fitting our ULXs with SIMPL \otimes DISKBB XSPEC emission model will help determine whether the observed soft excess is a feature of the ULX spectrum or the model.

Best fit SIMPL models are provided in Table 2; these include up-scattering and down-scattering. We reject all SIMPL fits to ULX3. We found acceptable fits for ULX1 and ULX2; however, the emission parameters could not be constrained. The best fit to ULX1 is presented in Fig. 5. F-testing tells us that we must prefer the two-component models, since they provided a lower χ^2 for the same degrees of freedom in each case, and this is always a significant improvement. We therefore infer that the soft excess is a genuine feature of ULX spectra; such a feature could be produced by an extended corona that has access to low energy photons from the outer disc.

¹ <http://heasarc.gsfc.nasa.gov/docs/xanadu/xspec/models/slimdisk.html>

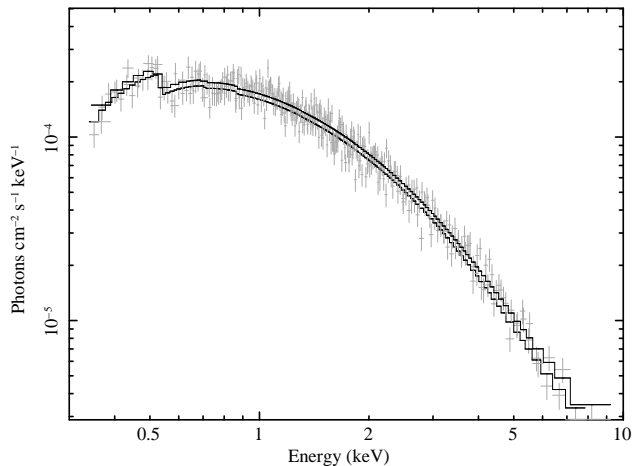


Figure 5. Unfolded 0.3–10 keV pn and combined MOS spectra of ULX1 with the best-fit SIMPL model. A constant of normalization accounts for the differences in pn and MOS responses.

One might expect the SIMPL and two component models to give equally acceptable results, as they are both describing the Comptonization of a disc blackbody, with no specified corona geometry. However, the SIMPL model does not include photons outside the energy range of the spectrum; hence, the softer photons in the cooler regions of the disc are excluded. We further note that the SIMPL model assumes that all photons have equal probability of being scattered, and that photons of all energies are scattered by the same amount (Steiner et al. 2008). The latter may approximate a compact corona, but is unlikely to be true for an extended corona, as the photon energies will vary by several orders of magnitude.

We also fitted SIMPL models to our XMM-Newton spectra for the known black hole + Wolf-Rayet binary IC10 X-1 (see Barnard et al. 2008a, and references within). The best fit model yielded $\chi^2/\text{dof} = 763/650$ (g.f.p. = 0.0014) and is rejected; the two component model yields $\chi^2/\text{dof} = 699/650$ (g.f.p. = 0.08). Hence we infer the soft excess to be a genuine feature of the IC10 X-1 emission spectrum also.

4 DISCUSSION AND CONCLUSIONS

ULX1 is a factor of ~ 3 times more variable than ULX2, despite the fact that ULX2 is brighter. Furthermore, the $\sim 0.0002\text{--}0.005$ Hz PDS of ULX1 is well described by $P(\nu) \propto \nu^{-1.0 \pm 0.5}$; the power at 0.0002 Hz is a factor ~ 10 higher than expected for the canonical low state for known black hole binaries (McClintock & Remillard 2006). However, the 0.0002 Hz power of ULX1 is consistent with the high state of Cygnus X-1 (Churazov et al. 2001). It is difficult to differentiate between the high state and very high state (a.k.a. steep power law state) using only the PDS (McClintock & Remillard 2006); however, the emission of ULX1 is more like the very high / steep power law state than the high state.

The best studied ULX spectra exhibit are well described by thermal + Comptonization emission models. They often exhibit soft excesses which have been labeled unphysical, assuming that the seed photons are provided by the inner disc (Roberts et al. 2005; Gonçalves & Soria 2006, e.g.). We have

tested this assumption using SIMPL models. We have rejected these models for ULX3 and IC10 X-1, and find that our two-component models are preferred for ULX1 and ULX2. We therefore infer that these soft excesses are genuine features of ULX spectra.

The disc blackbody contributes $1.3 \pm 0.2 \times 10^{39} \text{ erg s}^{-1}$ to the unabsorbed 0.3–10 keV flux from our best two-component fit to ULX1; a distance of 4 Mpc is assumed, but the distance is not well known. This is plausible for a black hole with mass $\sim 20 M_{\odot}$; the most massive known stellar mass black hole, in IC10 X-1, has a mass of $\sim 20\text{--}35 M_{\odot}$ (Silverman & Filippenko 2008).

We propose an explanation for the soft excess that crucially involves an extended corona. In Barnard et al. (2008a) we proposed that the canonical high soft state observed in the transient black hole binary systems is caused by the ejection of the disc corona as the X-ray luminosity increases by several orders of magnitude during outburst. We also proposed that a steady high accretion rate could maintain a stable corona, resulting in a non-thermal high state. This theory is supported by observations of the high mass black hole binary LMC X-1, which appears to be in a stable, non-thermal high state (Barnard et al. 2008a, and references within).

The “non-standard” fits to the ULXs resemble the emission generally seen in the Galactic X-ray binaries with neutron star primaries; White et al. (1988) found neutron star LMXB spectra to be dominated by a Comptonized emission component, with an additional blackbody component at high luminosities, while Church & Bałucińska-Church (2001) found that the blackbody component was present at low luminosities also. The thermal and non-thermal emission components are spatially distinct in the neutron star LMXBs, as demonstrated by the high inclination LMXBs known as the dipping sources where the X-ray source is experiences increased absorption by material in the outer accretion disc on the orbital period; the thermal component is completely and abruptly removed by dipping, while the Comptonized component experiences more gradual changes in absorption (see e.g. White & Swank 1982; Church & Bałucińska-Church 1995; Barnard et al. 2001).

Corona sizes can be estimated for high inclination X-ray binaries, from the ingress times of the intensity dips caused by photo-electric absorption of X-rays by cold material in the outer accretion disc (see e.g. Church 2001, for details). Measured corona diameters for the dipping sources range from 20,000 km to 700,000 km with radius increasing with luminosity (Church 2001; Church & Bałucińska-Church 2004); the measured coronae extend over 10–50% of the accretion disc radius, with this fraction increasing with luminosity. Such extended coronae would have access to an enormous reservoir of photons $\ll 1$ keV that could account for the soft excess.

We note that further, independent evidence for extended coronae has been discovered by Schulz et al. (2009). They found broadened emission lines in Chandra observations of Cygnus X-2, requiring Doppler velocities of $\sim 1100\text{--}2700 \text{ km s}^{-1}$. Schulz et al. (2009) infer from these results that the corona of Cygnus X-2 is hot, dense and extended up to $\sim 10^{10} \text{ cm}$.

If the coronae in ULXs are similarly extended, as our results suggest, then the Eddington limit may be relaxed

Table 2. Best fit self-consistent Comptonization models to the ULXs. The spectral model used was `CONST*WABS*SIMPL(DISKBB)` with `CONST` accounting for the differences in pn and MOS response. The models include up-scattering and down-scattering. We show the absorption ($N_{\text{H}}/10^{20}$ atom cm^{-2}), photon index (Γ), scattering fraction (f_{scat}), and inner disc temperature (kT_{in}). We then give the χ^2/dof and good fit probability. The emission parameters are unconstrained for all models.

Model	$N_{\text{H}}/10^{20}$ atom cm^{-2}	Γ	f_{scat}	kT_{in}	χ^2/dof [g.f.p]
ULX1	6	1.1	0.3	1.0	359/323 [0.08]
ULX2	16	3.2	0.6	1.3	386/374 [0.32]
ULX3	24	1.1	0.4	0.8	110/76 [7E-3]

and many observed ULXs may be explained by stellar mass black holes accreting at a consistently high rate, but radiating at a locally sub-Eddington level. We propose that the non-thermal component of the observed ULX spectrum is provided by an extended corona that Comptonizes photons from the inner regions of the disc: the hot photons from the inner disc and also cool photons from further out. The observed thermal component would then be the portion of the disc emission that is unscattered.

This state may well be related to the canonical very high / steep power law state. Indeed, if the high soft state is caused by ejection of the corona during transient outburst, then the very high state could indicate that the corona was regenerating; an extended corona could make the very high state appear brighter in X-rays than the high soft state if sufficient cool photons were inverse-Compton scattered into the observed energy range. It is unfortunate that the highest quality X-ray observations of Galactic black hole binaries, from RXTE, are insensitive to energies below 2 keV; sensitive spectra could reveal a soft excess, and extended corona, in the very high state also.

The extended corona scenario means that many ULXs could contain stellar mass black holes that exhibit a super-Eddington luminosity while being locally sub-Eddington. Furthermore, it may be directly tested, as IC10 X-1 is a high inclination system that eclipses on a ~ 35 hour period (Prestwich et al. 2007; Silverman & Filippenko 2008); if our scenario is correct, then we would observe photo-electric absorption dips on the orbital period, and could determine the size of its corona from the ingress time.

ACKNOWLEDGMENTS

We thank the anonymous referee for their constructive and informative comments. This work is based on observations with XMM-Newton, an ESA science mission with instruments and contributions directly funded by ESA member states and the US (NASA). Astronomy research at the Open University is funded by an STFC Rolling Grant.

REFERENCES

- Barnard, R., Bałucińska-Church, M., Smale, A. P., & Church, M. J. 2001, *A&A*, 380, 494
- Barnard, R., Clark, J. S., & Kolb, U. C. 2008a, *A&A*, 488, 697
- Barnard, R., Shaw Greening, L., & Kolb, U. 2008b, *MNRAS*, 388, 849
- Barnard, R., Trudolyubov, S., Kolb, U. C., et al. 2007, *A&A*, 469, 875
- Churazov, E., Gilfanov, M., & Revnivtsev, M. 2001, *MNRAS*, 321, 759
- Church, M. J. 2001, *Advances in Space Research*, 28, 323
- Church, M. J. & Bałucińska-Church, M. 2001, *A&A*, 369, 915
- Church, M. J. & Bałucińska-Church, M. 1995, *A&A*, 300, 441
- Church, M. J. & Bałucińska-Church, M. 2004, *MNRAS*, 348, 955
- Dewangan, G. C., Griffiths, R. E., & Rao, A. R. 2006a, *ApJL*, 641, L125
- Dewangan, G. C., Titarchuk, L., & Griffiths, R. E. 2006b, *ApJL*, 637, L21
- Gladstone, J. C., Roberts, T. P., & Done, C. 2009, *MNRAS*, 397, 1836
- Gonçalves, A. C. & Soria, R. 2006, *MNRAS*, 371, 673
- Grimm, H.-J., Gilfanov, M., & Sunyaev, R. 2003, *MNRAS*, 339, 793
- Heil, L. M., Vaughan, S., & Roberts, T. P. 2009, *ArXiv e-prints*
- Isobe, N., Makishima, K., Takahashi, H., et al. 2009, *PASJ*, 61, 279
- Kawaguchi, T. 2003, *ApJ*, 593, 69
- McClintock, J. E. & Remillard, R. A. 2006, *Compact stellar X-ray sources*, 157
- Mitsuda, K., Inoue, H., Koyama, K., et al. 1984, *PASJ*, 36, 741
- Okajima, T., Ebisawa, K., & Kawaguchi, T. 2006, *ApJL*, 652, L105
- Prestwich, A. H., Kilgard, R., Crowther, P. A., et al. 2007, *ApJL*, 669, L21
- Roberts, T. P. 2007, *Ap&SS*, 311, 203
- Roberts, T. P., Warwick, R. S., Ward, M. J., Goad, M. R., & Jenkins, L. P. 2005, *MNRAS*, 357, 1363
- Schulz, N. S., Huenemoerder, D. P., Ji, L., et al. 2009, *ApJL*, 692, L80
- Silverman, J. M. & Filippenko, A. V. 2008, *ApJL*, 678, L17
- Soria, R. & Kuncic, Z. 2008, in *American Institute of Physics Conference Series*, Vol. 1053, American Institute of Physics Conference Series, 103–110
- Steiner, J. F., Narayan, R., McClintock, J. E., & Ebisawa, K. 2008, *ArXiv e-prints*
- Stobart, A.-M., Roberts, T. P., & Wilms, J. 2006, *MNRAS*, 368, 397
- Strohmayer, T. E. & Mushotzky, R. F. 2003, *ApJL*, 586,

L61

Strohmayer, T. E., Mushotzky, R. F., Winter, L., et al.
2007, ApJ, 660, 580

White, N. E., Stella, L., & Parmar, A. N. 1988, ApJ, 324,
363

White, N. E. & Swank, J. H. 1982, ApJL, 253, L61